Physics Letters B 766 (2017) 86–93

Contents lists available at ScienceDirect

Physics Letters B

www.elsevier.com/locate/physletb

Minkowski space pion model inspired by lattice QCD running quark mass

Clayton S. Mello [a], J.P.B.C. de Melo [b], T. Frederico [a,*]

[a] Instituto Tecnológico de Aeronáutica, DCTA, 12.228-900 São José dos Campos, SP, Brazil
[b] Laboratório de Física Teórica e Computacional – LFTC, Universidade Cruzeiro do Sul, 01506-000 São Paulo, SP, Brazil

ARTICLE INFO

Article history:
Received 27 August 2016
Received in revised form 22 December 2016
Accepted 27 December 2016
Available online 2 January 2017
Editor: W. Haxton

Keywords:
Light-mesons
Bethe–Salpeter amplitude
Electromagnetic form factor
Decay constant
Constituent quark
Running mass

ABSTRACT

The pion structure in Minkowski space is described in terms of an analytic model of the Bethe–Salpeter amplitude combined with Euclidean Lattice QCD results. The model is physically motivated to take into account the running quark mass, which is fitted to Lattice QCD data. The pion pseudoscalar vertex is associated to the quark mass function, as dictated by dynamical chiral symmetry breaking requirements in the limit of vanishing current quark mass. The quark propagator is analyzed in terms of a spectral representation, and it shows a violation of the positivity constraints. The integral representation of the pion Bethe–Salpeter amplitude is also built. The pion space-like electromagnetic form factor is calculated with a quark electromagnetic current, which satisfies the Ward–Takahashi identity to ensure current conservation. The results for the form factor and weak decay constant are found to be consistent with the experimental data.

© 2016 Published by Elsevier B.V. This is an open access article under the CC BY license (http://creativecommons.org/licenses/by/4.0/). Funded by SCOAP[3].

1. Introduction

One fundamental goal of particle physics today, both in theory and experiments, is to explore the nonperturbative structure of hadrons. The accepted strong interaction theory is Quantum Chromodynamics (QCD) with quark and gluon degrees of freedom. Dedicated experiments are planned to investigate the nucleon structure with the 12 GeV JLAB upgrade [1], in particular focusing in the study of electromagnetic form factors, inclusive and semi-inclusive deep inelastic electron scattering. On the theory side, the research is devoted to the nonperturbative hadron properties from the strong interaction, which has being pursued in the Euclidean space by lattice QCD calculations (see e.g. [2–5]) and by Dyson–Schwinger methods in QCD (see e.g. [6]). In Minkowski space, the diagonalization of the Light-Front (LF) QCD hamiltonian [7], for example using the basis function approach forwarded by the Iowa group [8–14] gives, besides the spectrum, the hadron LF Fock-space wave function, explored through from factors, parton an generalized parton distributions. This effort demands a huge computational effort (see e.g. [8]) but is becoming nowadays more and more feasible. However, the study of the non-perturbative QCD with ab-initio methods is still very challenging. Therefore, phenomenological models are called for to explore the structure of hadrons waiting for more detailed ab-initio results.

Dynamical models that embed dynamical chiral symmetry breaking were indeed explored, as in [15], where the pion wave function from chiral quark models was extracted and compared to lattice QCD. In addition, the generalized quark transversity distribution of the pion was investigated [16]. Within the same spirit, but using the covariant spectator theory [17], it was studied in Minkowski space, confinement, the quark mass functions, spontaneous chiral symmetry breaking and the pion structure [18–20] in particular the pion electromagnetic form factor [21]. Further developments of the approach implements the complete charge-conjugation symmetry and evaluates the impulse approximation for the pion electromagnetic form factor [22]. Another example, of a recent nonperturbative approach to the pseudoscalar and vector meson spectrum in a light-front quark model within a variational treatment can be found in [23], and within a covariant approach of the Nambu and Jona-Lasinio model the pion transverse momentum dependent parton distributions was addressed in [24].

On the other side, there is the option to address directly the electroweak observables with light-front or covariant models, and the literature is quite rich and started long ago (see e.g. [25,26]), which despite their simplicity implement correctly kinematic boost properties of the corresponding amplitudes in exclusive processes [7]. Since sometime ago it is a common practice to study covariant and light-front models with constituent quark degrees of free-

* Corresponding author.
E-mail address: tobias@ita.br (T. Frederico).

http://dx.doi.org/10.1016/j.physletb.2016.12.058
0370-2693/© 2016 Published by Elsevier B.V. This is an open access article under the CC BY license (http://creativecommons.org/licenses/by/4.0/). Funded by SCOAP[3].

dom starting from an analytical form of the Bethe–Salpeter (BS) amplitude and with the Mandelstam formula compute the electromagnetic form factors, like in the case of the ρ-meson [27–29], for pseudoscalar mesons (see e.g. [30–33]), transition form factors between pseudoscalar and vector mesons [34] and generalized parton distributions [35,36]. A common feature of these models is a constituent quark mass independent of the momentum. On the other hand, Euclidean Lattice QCD calculations predict for the light quarks a running self-energy with momentum, which at infrared scales gives a value compatible with the constituent quark mass of about 0.3 GeV. Therefore, phenomenological models defined in Minkowski space could profit from using a running quark mass, with the proviso that it should be consistent with the ab-initio lattice QCD calculations on the Euclidean space for space-like momentum [37]. Progress in building the bridge between Euclidean and Minkowski space calculations have been achieved recently, namely, the pion light-front wave function was found from the dynamical chiral symmetry breaking [38], the distribution amplitude from lattice QCD results [39] and the pion electromagnetic form factor on the entire domain of space-like momentum transfer using the Dyson–Schwinger equation framework applied to QCD [40].

From the general point of view, integral representations of the two and three-point functions, i.e. the Källén–Lehmann spectral representation [41] and the Nakanishi integral representation [42] respectively, are an useful tool to enlarge the applicability of Euclidean calculations, like the ones obtained in lattice QCD to built the Minkowski space amplitudes. Indeed, recently it was used the Källén–Lehmann (KL) representation to obtain the spectral density from the lattice QCD gluon propagator in the space-like region through the solution of an ill-posed problem [43]. It was checked that the violation of the positivity constraint of the spectral density happens and the absence of gluons from the asymptotic spectrum of the theory. Similar conclusion was already found from the solution of Dyson–Schwinger equations for the gluon propagator [44]. With respect to the BS amplitude, the Nakanishi integral representation (NIR) allied to the light-front projection was applied to solve nonperturbative problems in the Minkowski space, as the bound state solution of the BS equation in scalar models [45,46], for two fermions [47] and the scattering [48,49]. It was also used to investigate the bound-state structure in Minkowski space starting from the BS amplitude [50], where in particular the analytic extension of the integral representation to the Euclidean space was carefully checked. It would be desirable to perform the study of hadron structure using the Nakanishi representation of the BS amplitude by extending Euclidean calculations to the Minkowski space with a gain in the understanding of the associated observables.

In this work, we focus on the pion structure in Minkowski space described in terms of an analytic model of the Bethe–Salpeter amplitude combined with Euclidean Lattice QCD results. The model takes into account the running quark mass, which will be fitted to Lattice QCD data for space-like momentum in the Landau gauge [37]. The mass function ansatz has a single pole form added to the current quark mass (see e.g. [51,52]), from that we build the quark propagator, which is analyzed through the KL spectral representation and we will show that the positivity constraints are violated. After that, the pion BS amplitude will be built relying on the pseudoscalar vertex component, which is directly associated to the quark mass function, as dictated by the dynamical chiral symmetry breaking requirements in the limit of vanishing current quark mass, due to the axial-vector Ward–Takahashi identity (see e.g. [6]). Furthermore, the Nakanishi integral representation of the pion Bethe–Salpeter amplitude considering the running quark mass will be derived, which generalizes the model proposed in [36]. The performance of the ansatz is tested against the experimental data for the pion decay constant and space-like electromagnetic form factor, and the quark electromagnetic current will be derived constrained by the Ward–Takahashi identity to ensure current conservation. The proposed ansatz goes beyond previous pion BS amplitude models [30,31,35,56,57] by taking into account the quark self-energy in the fermion–antifermion–pion vertex and in the quark propagators. We believe that improvement is important for further applications to compute Minkowski space observables associated to the pion light-front wave function, as the generalized parton distributions [36] and the transverse pion structure [24,58].

2. Quark model propagator

In general the quark propagator can be written as:

$$S_F(k) = \imath\, Z(k^2)\left[\not{k} - M(k^2) + \imath\epsilon\right]^{-1} \tag{1}$$

and it is gauge dependent, while the observables we computed are not. In addition, the dynamical mass function $M(k^2)$ is renormalization-point-independent (see e.g. [53]).

Our model is built to fit the quark propagator in the space-like region obtained from Lattice QCD calculations in the Landau gauge [37]. This choice is quite popular as it is a smooth gauge in the sense that preserves the Lorentz invariance of QCD. The lattice calculations from [37] have two degenerate light u and d quarks and a heavier one for the strange quark. This simulation used configurations from an improved staggered "Asqtad" action at β = 7.09, and our fit uses the result closest to the chiral limit among the light bare-quark mass calculations. As a simplification, we do not consider the momentum dependence of the quark wave function renormalization factor, $Z(k^2) = 1$, and the adopted dressed quark propagator is

$$S_F(k) = \imath\left[\not{k} - M(k^2) + \imath\epsilon\right]^{-1}. \tag{2}$$

This ansatz suggested long ago [59–62] simplifies our calculations of the pion electroweak observables in Minkowski space. We note that Lattice QCD results [37] shows some momentum dependence in $Z(k^2)$, that has a value of about 0.7 close to $k^2 = 0$. In addition we use the following mass function parametrization,

$$M(k^2) = m_0 - m^3\left[k^2 - \lambda^2 + i\epsilon\right]^{-1}, \tag{3}$$

already applied to fit Lattice QCD calculations [52]. The parameters of the running mass function are given by

$$m_0 = 0.014\ \text{GeV},\ \ m = 0.574\ \text{GeV and}\ \lambda = 0.846\ \text{GeV}, \tag{4}$$

which are close to the ones used in [52]. The parameters we use fit the experimental pion charge radius and provides f_π close to the experimental value, as we will present in our result section. The running quark mass function with our choice of parameters is shown in Fig. 1 and compared to Lattice QCD calculations [37]. We observe that our results are quite close to the lattice results considering the attributed errors. For comparison we also show the fit given in Ref. [51], with a more sophisticated parametrization including log's, which in the present model we didn't consider with the sake to simplify the loop integrations in Minkowski space associated with the pion electroweak observables.

The model has quark propagator poles for $m_i^2 = M^2(m_i^2)$ (i labels the pole position), which are given by solving the cubic equations:

$$m_i\left(m_i^2 - \lambda^2\right) = \pm\left[m_0\left(m_i^2 - \lambda^2\right) - m^3\right], \tag{5}$$

which allows to factorize the denominator of the quark model propagator as

$$S_F(k) = \imath\,\frac{\left(k^2-\lambda^2\right)^2\,(\not{k}+m_0)-\left(k^2-\lambda^2\right)m^3}{\prod_{i=1,3}(k^2-m_i^2+\imath\epsilon)}\,. \tag{6}$$

With the parameters given above, the poles are real and placed at the values of $m_1 = 0.327$ GeV, $m_2 = 0.644$ GeV and $m_3 = 0.954$ GeV. Although the quark model propagator has real poles, and m_1 resembles the constituent mass, or alternatively $M(k^2=0) = m_0 + m^3/\lambda^2 = 0.278$ GeV. It is worthwhile to stress that quark confinement is associated with the absence of asymptotic states of free quarks in QCD. Such physics is suggested to be expressed as pair of poles of the quark propagator that have migrated to the complex plane (see e.g. the review [6]). Despite of that, we will proceed with this simplified model, which is quite practical for building the pion observables in Minkowski space, namely the loop integrations associated with the observables are easily performed analytically.

The fermion propagator can be written as

$$S_F(k) = \imath\left[A(k^2)\not{k} + B(k^2)\right]. \tag{7}$$

The spectral decomposition [41]:

$$A(k^2) = \int_0^\infty d\mu^2 \frac{\rho_A(\mu^2)}{k^2-\mu^2+\imath\varepsilon} \quad \text{and} \quad B(k^2) = \int_0^\infty d\mu^2 \frac{\rho_B(\mu^2)}{k^2-\mu^2+\imath\varepsilon} \tag{8}$$

where the spectral densities are:

$$\rho_A(\mu^2) = -\frac{1}{\pi}\,\mathrm{Im}\left[A(\mu^2)\right] \quad \text{and} \quad \rho_B(\mu^2) = -\frac{1}{\pi}\,\mathrm{Im}\left[B(\mu^2)\right] \tag{9}$$

For a particle that belongs to the S-matrix representation, which is an observable state, the Källén–Lehmann (KL) spectral densities satisfy the positivity constraints [41]:

$$\mathcal{P}_a = \rho_A(\mu^2) \geq 0 \quad \text{and} \quad \mathcal{P}_b = \mu\,\rho_A(\mu^2) - \rho_B(\mu^2) \geq 0\,. \tag{10}$$

The quark is a non-singlet color state and it is not an observable asymptotic state belonging to the S-matrix representation. Thus, there is no guarantee that the quark propagator should have a KL representation. If it will be possible to have one, it might violate the positivity constraints for the spectral density. However, this is not a simple issue as the positivity violation is a sufficient but not necessary condition for quark confinement (see e.g. [54]). Then, positivity violation associated with the quark propagator may not be equivalent to confinement, which is a subtle property to define in presence of dynamical quarks [55]. In addition, the issue of physical or nonphysical asymptotic states must be associated with the gauge-singlet properties of the object, that excludes of course the quarks as being an observable state. In this context, we warn the reader that, our phenomenological model does not explicitly resolve the issue of quark confinement, like e.g. the confining force between the quark-antiquark, beyond the observation that the quark spectral density in the present case is not positive definite, as we are going to show. A similar quark propagator model, proposed recently, violates the reflection positivity and was associated to quarks degrees of freedom out of the physical spectrum [52]. The detailed discussion presented in this reference is particularly illuminating on that point. We can add the example of the gluon propagator obtained from Lattice QCD calculations in the Landau gauge, which exhibits the violation of the positivity constraint in the KL representation [43].

For our model we can compute easily the spectral densities by decomposing, the quark model propagator (6), first in partial fractions as:

$$A(k^2) = \frac{H_2(m_1,m_2,m_3)}{k^2-m_1^2+\imath\epsilon} + \frac{H_2(m_2,m_1,m_3)}{k^2-m_2^2+\imath\epsilon} + \frac{H_2(m_3,m_2,m_1)}{k^2-m_3^2+\imath\epsilon} \tag{11}$$

and

$$B(k^2) = \frac{H_1(m_1,m_2,m_3)}{k^2-m_1^2+\imath\epsilon} + \frac{H_1(m_2,m_1,m_3)}{k^2-m_2^2+\imath\epsilon} + \frac{H_1(m_3,m_2,m_1)}{k^2-m_3^2+\imath\epsilon} + m_0\,A(k^2) \tag{12}$$

where

$$H_n(m_1,m_2,m_3) = \frac{(-m^3)^{2-n}(m_1^2-\lambda^2)^n}{(m_1^2-m_2^2)(m_1^2-m_3^2)} \tag{13}$$

which leads easily leads to:

$$\begin{aligned}\rho_A(\mu^2) = {} & H_2(m_1,m_2,m_3)\;\delta\left(\mu^2-m_1^2\right) \\ & + H_2(m_2,m_1,m_3)\;\delta\left(\mu^2-m_2^2\right) \\ & + H_2(m_3,m_2,m_1)\;\delta\left(\mu^2-m_3^2\right)\end{aligned} \tag{14}$$

and

$$\begin{aligned}\rho_B(\mu^2) = {} & H_1(m_1,m_2,m_3)\;\delta\left(\mu^2-m_1^2\right) \\ & + H_1(m_2,m_1,m_3)\;\delta\left(\mu^2-m_2^2\right) \\ & + H_1(m_3,m_2,m_1)\;\delta\left(\mu^2-m_3^2\right) + m_0\,\rho_A(\mu^2)\end{aligned} \tag{15}$$

The constraints in (10) are translated to the coefficients of the delta functions, which using (14) and (15) are given by:

$$\begin{aligned}&\mathcal{P}_a^\delta(m_1,m_2,m_3) = H_2(m_1,m_2,m_3) \;\text{ and} \\ &\mathcal{P}_b^\delta(m_1,m_2,m_3) = H_1(m_1,m_2,m_3) + m_0\,H_2(m_1,m_2,m_3)\,.\end{aligned} \tag{16}$$

As $m_1 < m_2 < m_3$, one has that $\mathcal{P}_a^\delta(m_2,m_1,m_3) < 0$ and $\rho_A(\mu^2)|_{\mu^2=m_2^2} < 0$. The actual values are $\mathcal{P}_a^\delta(m_1,m_2,m_3) = 1.49$, $\mathcal{P}_a^\delta(m_2,m_1,m_3) = -0.580$ and $\mathcal{P}_a^\delta(m_3,m_2,m_1) = 0.095$.

The other positivity constraint from (10), translated into the coefficients of the delta functions turns to be:

$$\mathcal{P}_b^\delta(m_1,m_2,m_3) = -\frac{(\lambda^2-m_1^2)(m^3+(m_0-m_1)(\lambda^2-m_1^2))}{(m_1^2-m_2^2)(m_1^2-m_3^2)}\,. \tag{17}$$

The formula above has to be calculated for each one of the three poles of the quark propagators, namely m_1, $m_1 \leftrightarrow m_2$ and $m_1 \leftrightarrow m_3$. Taking into account the actual values of the poles and parameters it results: $\mathcal{P}_b^\delta(m_1,m_2,m_3) \sim -0.001$, $\mathcal{P}_b^\delta(m_2,m_1,m_3) \sim 0.001$ and $\mathcal{P}_b^\delta(m_3,m_2,m_1) = 0.183$. In short, we found that the model violates the positivity constraints for the spectral density and we are satisfied by that as the color non-singlet quark cannot be a physical state.

3. Pion Bethe–Salpeter amplitude model

The pion is a isovector pseudoscalar meson composed mainly by a constituent quark and antiquark, i.e., $|u\,\bar{d}\rangle$ state with total spin zero and negative parity. The key ingredient of the model is the chiral limit where the current quark mass vanishes and the self-energy is related to the pion BS vertex.

The pion-quark-antiquark vertex denoted by $\Gamma_\pi(k,P)$ is the quark-antiquark-meson BSA with external quark legs removed. In

the isovector and pseudoscalar channel the BS vertex has the general form:

$$\Gamma_\pi(k;P) = \gamma_5[\imath E_\pi(k;P) + \not{P} F_\pi(k;P) + k^\mu P_\mu \not{k} G_\pi(k;P) + \sigma_{\mu\nu} k^\mu P^\nu H_\pi(k;P)], \quad (18)$$

where $P^2 = m_\pi^2$. In our calculations we consider the chiral limit, where the current quark mass vanishes and $m_\pi = 0$. In this case the pion vertex can be written as (see e.g. [6,38]):

$$f_\pi E_\pi(k,P) = M(k^2)/\sqrt{Z(k^2)}, \quad (19)$$

where f_π is the pion electroweak decay constant and only the scalar part of the quark self-energy appears in the above equality.

The present model for the pion BSA, which incorporates the effects from quark dressing and dynamical chiral symmetry breaking, through the running mass, is written as:

$$\psi_\pi(k;P) = S_F(k+P/2)\,\Gamma_\pi(k;P)\,S_F(k-P/2), \quad (20)$$

where the quarks are in a colorless state and k is the relative momentum.

We consider the chiral limit, namely the current quark mass vanishes ($m_0 = 0$) and $m_\pi = 0$, where only the contribution of the pseudoscalar Dirac matrix survives in the vertex, which simplifies even further the model, giving that

$$\Gamma_\pi(k;P) = \imath\,\mathcal{N}\,\gamma_5\,M(k^2)|_{m_0=0}, \quad (21)$$

where $\mathcal{N}$ is the normalization constant found by imposing that the electromagnetic form factor is 1 for zero momentum transfer. Then, introducing the factorized form of the quark propagator (6) and the vertex function (21) in the pion BSA (20), the present model reads:

$$\psi_\pi(k;P) = -\frac{\left((k+\frac{P}{2})^2-\lambda^2\right)^2 (\not{k}+\frac{\not{P}}{2}+m_0) - \left((k+\frac{P}{2})^2-\lambda^2\right) m^3}{\prod_{i=1,3}((k+\frac{P}{2})^2 - m_i^2 + \imath\epsilon)} \times \frac{\mathcal{N}\gamma_5 m^3}{k^2-\lambda^2+\imath\epsilon} \times \frac{\left((k-\frac{P}{2})^2-\lambda^2\right)^2 (\not{k}-\frac{\not{P}}{2}+m_0) - \left((k-\frac{P}{2})^2-\lambda^2\right) m^3}{\prod_{i=1,3}((k-\frac{P}{2})^2 - m_i^2 + \imath\epsilon)}. \quad (22)$$

The position of the time-like poles, namely m_i are computed from the model parameters m, m_0 and λ, determined from the fit to the LQCD results for the running quark mass for space-like momentum, as shown in Fig. 1.

We point out that the choice of the vertex function (21) turns the loop integrals for the electromagnetic form factor and decay constant finite, and eliminates the log-type divergences for ultraviolet momentum, which appear when the quark mass and vertex go to constant values. Although the running mass of the quark goes to m_0 for large momentum, the vertex function decreases fast enough as $\sim 1/k^2$, which kills the log-type divergence in the loop integrals.

One should compare with previous models of the pion BSA from [31,35,36]. These pion models are summarized by the formula:

$$\psi_\pi(k;P) = -\frac{\not{k}+\frac{\not{P}}{2}+M_q}{(k+\frac{P}{2})^2 - M_q^2 + \imath\epsilon}\,\gamma_5\,\Lambda_\pi(k,P) \times \frac{\not{k}-\frac{\not{P}}{2}+M_q}{(k-\frac{P}{2})^2 - M_q^2 + \imath\epsilon}, \quad (23)$$

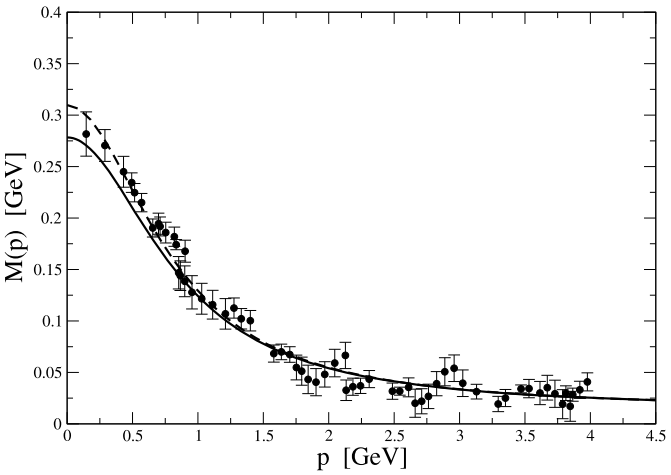

Fig. 1. The running quark mass, Eq. (3), as a function of the Euclidean momentum $p = \sqrt{-p^\mu p_\mu}$, with parameters from (4), is given by the solid line and compared to lattice QCD calculations from [37]. The dashed line shows the parametrization used in reference [51].

where M_q is a constituent quark mass, and the momentum component of the vertex, $\Lambda_\pi(k,P)$ is defined in terms of Pauli–Villars regulators:

$$\Lambda_\pi(k,P) = \mathcal{N}\left[\frac{1}{(k+\frac{P}{2})^2 - m_R^2 + \imath\epsilon} + \frac{1}{(k-\frac{P}{2})^2 - m_R^2 + \imath\epsilon}\right] \quad (24)$$

for the ansatz from Ref. [31], and

$$\Lambda_\pi(k,P) = \mathcal{N}\,\frac{1}{\left[(k+\frac{P}{2})^2 - m_R^2 + \imath\epsilon\right]}\,\frac{1}{\left[(k-\frac{P}{2})^2 - m_R^2 + \imath\epsilon\right]} \quad (25)$$

for the product ansatz used in Ref. [35] and recently in [36] to compute the pion generalized parton distributions.

It is worthwhile to point out that the Nakanishi integral representation [42] was used as a tool to explore the bound-state solution of the Bethe–Salpeter equation for bosons ground state [45,46] and excited states [50], for bound state of fermions [47] and continuum [48,49].

4. Integral representation of the BSA

In order to introduce the integral representation for our model, we use the following useful identity:

$$\frac{1}{((k+\frac{P}{2})^2 - \mu'^2 + \imath\epsilon)(k^2-\lambda^2+\imath\epsilon)((k-\frac{P}{2})^2 - \mu^2 + \imath\epsilon)} = \int_{-\infty}^{+\infty} d\gamma \int_{-1}^{1} dz \frac{g(\gamma,z;\mu',\mu,p)}{\left(k^2 + z\,k\cdot p + \gamma + \imath\epsilon\right)^3} \quad (26)$$

where

$$g(\gamma,z;\mu',\mu,p) = \frac{\theta(\alpha)\theta(1-\alpha)}{\frac{1}{2}-\alpha}\left[\theta(1-2\alpha-z)\theta(z) - \theta(z-1+2\alpha)\theta(-z)\right] \quad (27)$$

and

$$\alpha = \frac{\frac{p^2}{4} + \lambda^2 - \mu^2 - z^{-1}(\lambda^2+\gamma)}{\mu^2 - \mu'^2 + 2z^{-1}(\lambda^2+\gamma)}. \quad (28)$$

The support in γ bounded from below and it is implicitly given by the theta's in α as expressed by the formula (27).

The pion BS amplitude can be written alternatively as:

$$\psi_\pi(k;P) = -\left[A(k_q^2)\not{k}_q + B(k_q^2)\right]\frac{\mathcal{N}\gamma_5}{k^2-\lambda^2+\imath\epsilon} \times \left[A(k_{\bar{q}}^2)\not{k}_{\bar{q}} + B(k_{\bar{q}}^2)\right], \quad (29)$$

where $k_q = k + P/2$ and $k_{\bar{q}} = k - P/2$. Noting that the quark propagator model can be written via the spectral representation given in Eqs. (8), where the denominator has a simple form one can easily manipulate the BS amplitude (29) to have it written as in the elegant Nakanishi integral representation form. Four terms with the form given by the auxiliary identity (26) appear and one can write that:

$$\psi_\pi(k;P) = \gamma_5\,\chi_1(k,P) + \not{k}_q\,\gamma_5\,\chi_2(k,P) + \gamma_5\not{k}_{\bar{q}}\,\chi_3(k,P) + \not{k}_q\,\gamma_5\not{k}_{\bar{q}}\,\chi_4(k,P), \quad (30)$$

where

$$\chi_i(k,P) = \int_{-\infty}^{+\infty} d\gamma \int_{-1}^{1} dz \frac{g_i(\gamma,z;p)}{\left(k^2 + zk\cdot p + \gamma + \imath\epsilon\right)^3}. \quad (31)$$

The Nakanishi weight functions given by:

$$g_i(\gamma,z;p) = -\mathcal{N}\int_0^\infty d\mu^2 \int_0^\infty d\mu'^2 \rho_{C_i'}(\mu'^2)\rho_{C_i}(\mu^2)\, g(\gamma,z;\mu',\mu,p), \quad (32)$$

where $(C_1', C_1) = (B,B)$, $(C_2', C_2) = (A,B)$, $(C_3', C_3) = (B,A)$ and $(C_4', C_4) = (A,A)$. Although we have expressed the Nakanishi integral representation with Eq. (31), the support in γ is bounded from below (cf. Eq. (27)). The four terms of the BSA (30) can be rewritten with standard orthogonal Dirac operators, which was already used to solve the BS equation in ladder approximation [47].

5. Electroweak decay constant

Another relevant quantity to be used study our model is the pion decay constant, f_π. It is defined through the matrix element of the partially conserved axial-vector current, $\langle 0|A_i^\mu|\pi_j\rangle = \imath P^\mu f_\pi \delta_{ij}$. Following Ref. [26], we take $A_i^\mu = \bar{q}\gamma^\mu\gamma^5\frac{\tau_i}{2}q$, and our model (29) for the pion BSA. After the color and isospin algebra, one finds the following expression for the decay constant:

$$P^\mu f_\pi = N_c \int \frac{d^4k}{(2\pi)^4}\mathrm{Tr}\left[\gamma^\mu\gamma^5\psi_\pi(k;P)\right], \quad (33)$$

where N_c is the number of colors. Technically, we performed first the integration on $k^- = k^0 - k^3$ and choose the plus component of the axial current ($A_i^+ = A_i^0 + A_i^3$). In this way the formula for the decay constant can also be written in terms of the valence component of the light-front wave function of our model (see e.g. [7,31]).

6. Electromagnetic form factor

The pion composite structure from the nonperturbative physics of confinement and DCSB, which are incorporated in our model, are revealed in the elastic electromagnetic form factor. The meson-photon vertex is computed with the impulse approximation, where it is used the pion BSA model (29), the quark propagator (2) with a running mass (3) fitted to lattice QCD calculations. The impulse approximation to the pion-photon vertex makes evident the main elements of our model. In physical terms, in the impulse approximation the photon probes nonperturbatively either the dressed quark or the dressed antiquark in the pion.

We denote the general pion-photon vertex by $\Gamma_\pi^\mu(P,P';q)$, where P and P' are, respectively, the initial and final meson momenta, and $q = P' - P$ is the momentum transfer carried by the virtual photon. The pion-photon vertex is thus given by:

$$-\imath\,\Gamma_\pi^\mu(P,P';q) \equiv \langle\pi(P')|\,J^\mu\,|\pi(P)\rangle = (P+P')^\mu F_\pi(Q^2), \quad (34)$$

where $Q^2 = -q^2$, $|\pi(P)\rangle$ is the pion state and J^μ the electromagnetic current operator.

The building blocks of the impulse approximation are: (i) the nonperturbative quark-photon vertex $\Gamma_q^\mu(k',k;q)$ with $q = k' - k$, namely the dressed quark current; (ii) the dressed quark and antiquark propagators; and (iii) the pion-quark vertex. In the impulse approximation, the meson-photon vertex is written as the sum of two terms,

$$\Gamma_{\pi^+}^\mu(P,P';q) = \hat{Q}_u\Gamma_{\pi^+,u}^\mu(P,P';q) + \hat{Q}_{\bar{d}}\Gamma_{\pi^+,\bar{d}}^\mu(P,P';q), \quad (35)$$

where $\Gamma_{\pi^+,u}^\mu(P,P';q)$ is the contribution to the pion-photon vertex from the coupling of the photon with the up quark and $\Gamma_{\pi^+,\bar{d}}^\mu(P,P';q)$ comes from the down quark. The electromagnetic charges are $\hat{Q}_u$ and $\hat{Q}_{\bar{d}}$. Using appropriate momentum labelling, $\Gamma_{\pi^+,u}^\mu(P,P';q)$ is given by:

$$\Gamma_{\pi^+,u}^\mu(P,P';q) = N_c\int\frac{d^4k}{(2\pi)^4}\mathrm{Tr}\big[S_F(k'-P'/2)\bar{\Gamma}_{\pi^+}(k';P')S_F(k'+P'/2) \times \Gamma_u^\mu(k'+P'/2,k+P/2;P)S_F(k+P/2)\Gamma_{\pi^+}(k;P)\big], \quad (36)$$

where k is the loop integration variable, $k' = k + q/2$ and the trace is performed over Dirac indices. The final pion state is described by the vertex function $\bar{\Gamma}_{\pi^+}(k;P) = \Gamma_{\pi^+}(k;-P')$. A similar expression for $\Gamma_{\pi^+,\bar{d}}^\mu(P,P';q)$ can be written down. In the isospin symmetric limit ($m_u = m_{\bar{d}}$) it follows that:

$$\Gamma_{\pi,u}^\mu(P,P';q) = \Gamma_{\pi,\bar{d}}^\mu(P,P';q), \quad (37)$$

and therefore in our model there is only one independent quark electromagnetic vertex.

7. Dressed quark current operator

The conservation of the electromagnetic current is a fundamental physical constraint that model has to fulfill. The form of the meson-photon vertex and its form factor should reflect such constraint, which requires that $q_\mu\Gamma_\pi^\mu(P,P';q) = 0$, besides the normalization condition $\Gamma_\pi^\mu(P,P;q=0) = 2\,\imath\,P^\mu$. Therefore, the individual quark and antiquark contributions, Eq. (35), has to satisfy

$$\Gamma_{\pi^+,u}^\mu(P,P;q=0) = \Gamma_{\pi^+,\bar{d}}^\mu(P,P;q=0) = 2\,\imath\,P^\mu \text{ and}$$
$$q_\mu\Gamma_{\pi^+,u}^\mu(P,P';q) = q_\mu\Gamma_{\pi^+,\bar{d}}^\mu(P,P';q) = 0. \quad (38)$$

The impulse approximation preserves the electromagnetic current conservation automatically, Eq. (38), provided that the quark-photon vertex satisfies the Ward–Takahashi identity (WTI) [63–65]:

$$q_\mu\Gamma_q^\mu(p',p;q) = S_F^{-1}(p') - S_F^{-1}(p), \quad (39)$$

where the dressed quark propagator is given by Eq. (2). Simple manipulation of the WTI above, allows to isolate the quark-photon vertex:

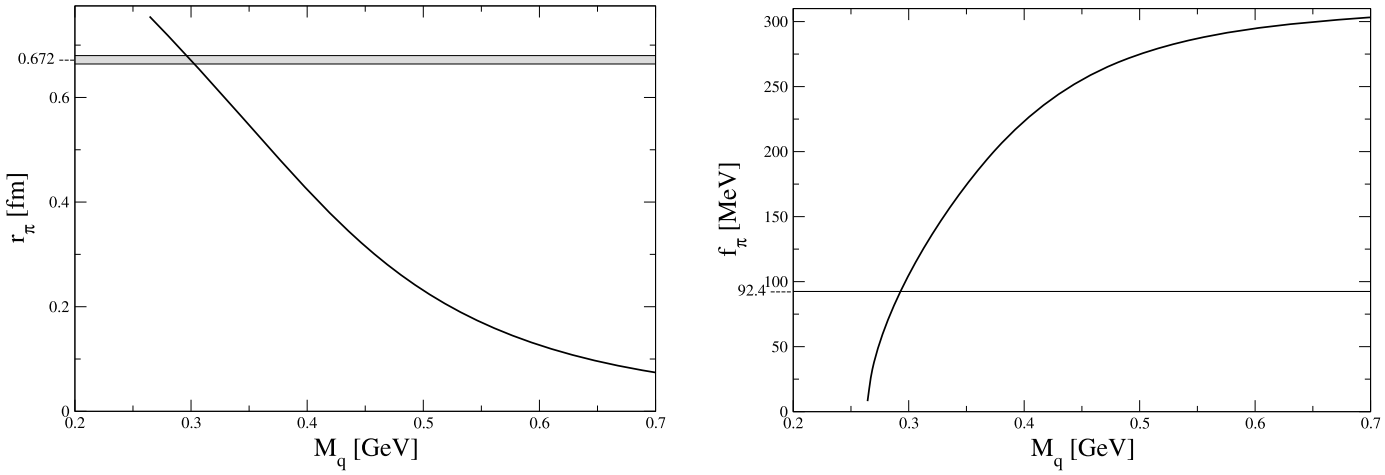

Fig. 2. Pion charge radius (left-frame) and decay constant (right-frame) as a function of the quark mass given for $M_q \equiv M\left(k^2=0\right)$. The experimental data for the charge radius and decay constant [67] are given by the horizontal lines.

$$-\imath\,\Gamma^{\mu}_{q}(p',p;q) = \gamma^{\mu} - \frac{m^3(p'+p)^{\mu}}{\mathcal{D}(p'^2)\mathcal{D}(p^2)}\,, \tag{40}$$

where the denominator is defined by the function $\mathcal{D}(p^2) = \left(p^2-\lambda^2+i\epsilon\right)$ and $q=p'-p$ is the incoming photon momenta. The general form of the quark-photon satisfies the WTI, Lorentz symmetry, and the correct perturbative limit in the ultraviolet limit. We expect that with the BSA from (29) and the quark-photon vertex given above, the asymptotic power-law ultraviolet behavior of the pion form factor as predicted in QCD [7] could be recovered.

8. Results

The pion electroweak observables are obtained from Eq. (33) for f_π and from Eq. (36) for the pion electromagnetic form factor with the quark-photon vertex (40) satisfying the WTI with the quark propagator (2) to ensure current conservation. The pion Bethe–Salpeter amplitude is given by (29) and the normalization factor, $\mathcal{N}$, is obtained from the condition that $F_\pi(0)=1$. In the actual calculations we use $m_\pi = 138$ MeV.

Our framework allows to compute the loop integrals in Minkowski space and technically we perform the analytical integrations with light-front momentum. We use the plus components of the axial-vector and vector currents to obtain the pion decay constant and form factor, respectively. The Breit-frame with the Drell–Yan condition ($q^+ = q^0+q^3=0$) is chosen to compute the pion form factor, which maximally avoids contributions from end-points or Z-diagrams in the limit of $q^+\to 0$ (see e.g. [30] and for a recent discussion [66]). The integration over the light-front energy $k^- := k^0-k^3$ is performed analytically via the Cauchy residue theorem, and we checked that our model has no end-point contributions for the plus components of the axial-vector and vector currents. The remaining integrations in $k^+ = k^0+k^3$ and $\mathbf{k}_\perp \equiv k_x, k_y$ are performed numerically.

The choice of parameters for the quark mass function given in (4) provides $r_\pi = 0.672$ fm, $f_\pi = 90$ MeV and the dimensionless product $r_\pi\, f_\pi = 0.306$ compared to the experimental values of $r_\pi^{exp} = 0.672 \pm 0.008$ fm [67], $f_\pi^{exp} = 92.42 \pm 0.021$ MeV [67] and $r_\pi^{exp}\, f_\pi^{exp} = 0.315 \pm 0.04$. Next, we allow some variation on the value of the scale parameter m, which moves the quark mass given by $M_q \equiv M\left(k^2=0\right)$ to study the sensitivity of r_π and f_π to the model scale. This parameter in the running mass formula (3) is changed, while the other two are fixed in the calculations.

In Fig. 2, the results for the pion charge radius and decay constant are shown as function of the quark mass, M_q, and compared with the experimental data. We observe that the radius decreases with M_q, naturally due to the relative increase of the mass scale and the concomitant decrease of the length scale by $\Delta M_q/M_q \sim -\Delta r_\pi/r_\pi$, which can be checked by the results in the left-frame of the figure. Then, the decrease of the pion radius, is related to the increase of the binding, when the mass increases for a fixed pion mass. At the same time the model has a simultaneous increase of f_π with the quark mass, as naively the $q\bar{q}$ pair tends to be in a more compact configuration with the increase of the probability for the pair to overlap, which leads to a qualitative consistence with the relation $r_\pi\, f_\pi = \sqrt{N_c}/2\pi$ [68,69], obtained in the limit of a constant quark-pion vertex. We remind that, relativistic constituent quark models approximately verifies this relation (see e.g. [26]) as well as for the pion obtained within Dyson–Schwinger calculations (see e.g. [6]).

In Fig. 3, we present the numerical calculations of the pion form factor F_π using our pion BS amplitude model from Eq. (22) and compare to the experimental data [70–75]. The bare quark-antiquark-photon vertex, $\Gamma^{\mu}(p,k;q) = \imath\,\gamma^{\mu}$, is inappropriate since it violates current conservation as expressed by the Ward–Takahashi identity, namely Eq. (39), with the dressed quark propagator. We enforced the WTI by building a quark electromagnetic current that satisfies Eq. (39) with the model dressed quark propagator from Eq. (2). That results in the non-trivial quark-photon vertex given by Eq. (40), that carries the momentum scale $\lambda = 0.846$ GeV associated with the nonperturbative QCD physics contained in the mass function for the space-like momentum. The magnitude of the chiral symmetry breaking is associated with the constituent quark mass $M_q = M(k^2=0) \sim 0.3$ GeV. This mass scale and λ are the essential information that constraint the quark current, pion BSA and consequently the electroweak observables.

Although the inclusion of the self-energy in the vertex conserves electromagnetic current via the vector WTI, the role of the vector meson excitations mixing with the photon seems less evident in the model. We just mention that in the time-like region the virtual photon can break into pair of quark and antiquark, which has the threshold given by the sum of two poles of the quark propagator, and with respect to the lower masses is $2\,m_1 = 0.646$ GeV, pretty close to the ρ meson mass of 0.776 GeV. On the other hand, this points to the limitation of the model, where no individual propagation of the vector meson or width can be clearly seen contributing to the form factor, as has been introduced in a previous light-front quark model of the pion [56,57].

The model assumed the quark wave function renormalization equal to one, while the results from the Lattice QCD calculations

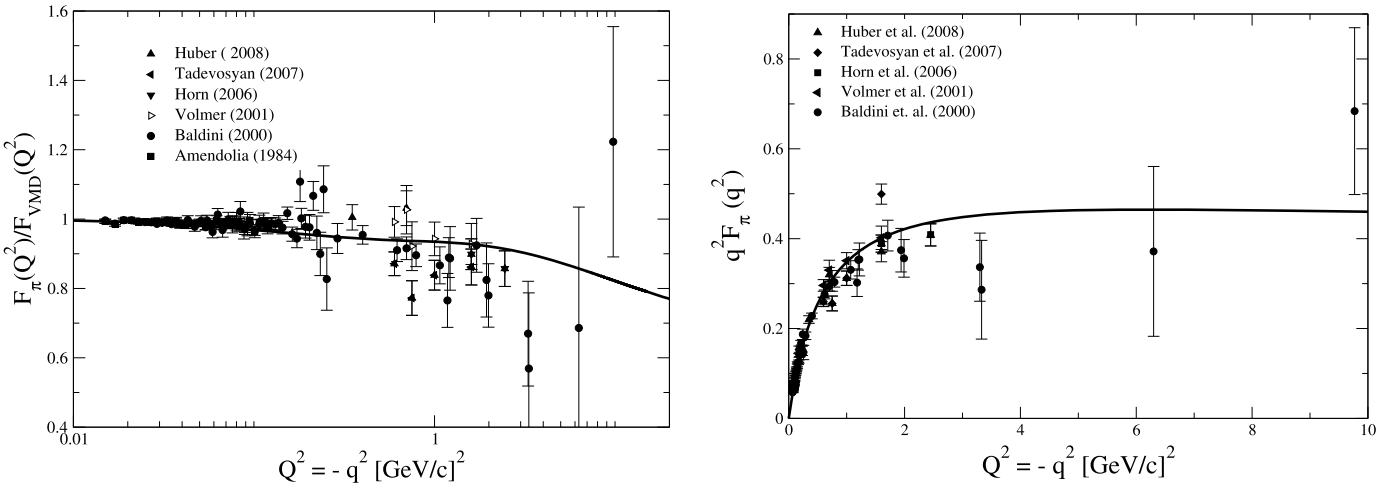

Fig. 3. Pion model electromagnetic form factor as a function of the space-like momentum transfer, $Q^2 = -q^2$, compared to the experimental values: Amendolia et al. [70], Baldini et al. [71], Volmer et al. [72], Horn et al. [73], Tadevosyan et al. [74] Huber et al. [75]. In the left frame it is presented the results normalized to the dipole form factor, $F_\pi(Q^2)(1 + Q^2/(0.77\ \text{GeV})^2)$, and in the right frame $Q^2F_\pi(Q^2)$.

in the Landau gauge [37] show $Z(k^2)$ about 0.7 at low momentum, $Z(k^2) \sim 0.9$ at 1 GeV and monotonically increases to one in the ultraviolet region. The net effect of the quark wave function renormalization is to damp the propagator in the infrared. This property should be reflected in the form factor, which is normalized to the pion charge. The main contribution to the integrand of the form factor expression, Eq. (36), comes from the loop integral in the low momentum region, therefore the quark wave function renormalization will enhance the relative importance of the integrand in the ultraviolet region with respect to the infrared one. As the form factor integrand goes as $\sim k^{-7}$ in the ultraviolet region and considering the charge normalization, we expect that the effect of $Z(k^2)$ will be washed out for low-momentum transfers, as well as for the decay constant. However, when the momentum transfer is large the form factor goes as $\sim q^{-2}$ (cf. Fig. 3) suggesting the company of a factor $Z(q^2)$, which would be reflected in a slight increase of the results compared to the one we showed. In this respect it will be desirable to have data with smaller errors, then the ones available for large momentum transfers.

9. Summary

The Minkowski space Bethe–Salpeter amplitude for the pion is introduced, based on a model of the quark propagator with self-energy. The model deals only with a running quark mass, that in the chiral limit, namely zero current quark mass, due to the axial-vector Ward–Takahashi identity is associated with the pseudoscalar component of the vertex function (see e.g. [6]). In this case our ansatz for the vertex function is the mass function, apart a normalization factor. The running quark mass model [52] has three parameters obtained from the fit to the Euclidean Lattice QCD results in the space-like momentum region [37]. The quark mass function has a single pole in the time like region at 0.846 GeV, includes a current quark mass of 0.014 GeV, and a third scale parameter that provides the value of the quark mass at zero momentum of 0.278 GeV. The quark propagator with the mass function model was decomposed in a form with three single poles, one is placed close to the constituent quark mass, and the other two poles are about two and three times the constituent quark mass. The Källén–Lehmann spectral decomposition of the quark propagator was analyzed, and we verified that the positivity constraints for the spectral densities are violated. This fact is minimally satisfactory suggesting that the model has a quark that should not correspond to a physical state.

The Nakanishi integral representation [42] of the BS amplitude model was worked out, and the corresponding weight function derived including both the structure of the vertex and the quark self-energy. This generalizes the discussion presented in [36] and introduces the model in the perspective of the recent applications of the integral representation to solve the bound state Bethe–Salpeter equation in Minkowski space (see e.g. [50]).

The quantitative performance of the model was checked against the pion electroweak observables, namely the decay constant and pion space-like electromagnetic form factor. In the last case, to ensure current conservation, the quark electromagnetic current was constructed from the self-energy in order to fulfill the Ward–Takahashi identity. Technically, we used the light-front momentum variables with the plus component of the axial-vector and vector currents to extract the weak decay constant and form factor with the Drell–Yan condition ($q^+ = 0$). The plus component of both axial-vector and electromagnetic current are free of zero mode contributions (see e.g. [30]), which simplified our calculations. The resulting form factor and decay constant computed in Minkowski space are consistent with the experimental data.

The proposed ansatz generalizes previous models of the pion Bethe–Salpeter amplitude [30,31,35,36,57] by taking into account the quark self-energy in the fermion–antifermion–pion vertex and in the quark propagators, important for further applications to compute generalized parton distributions [36] and also the transverse pion structure [24,58]. In addition the present model provides further insights on the valence wave function of the pion, which is extracted from the integral representation by projecting the BS amplitude on to the light-front (see e.g. [76,47]), allowing to access the rich body of parton distribution functions, envisaged in future applications.

Acknowledgements

The authors thank Giovanni Salmè and Orlando Oliveira for useful discussions. This work was partly supported by the Fundação de Amparo à Pesquisa do Estado de São Paulo (FAPESP) [grant nos. 2015/16295-5 and 2013/26258-4], Conselho Nacional de Desenvolvimento Científico e Tecnológico (CNPq) [grant nos. 308025/2015-6 and 308486/2015-3] and Coordenação de Aperfeiçoamento de Pessoal de Nível Superior (CAPES) of Brazil.

References

[1] J. Dudek, et al., Eur. Phys. J. A 48 (2012) 187.
[2] I. Montvay, G. Münster (Eds.), Quantum Fields on a Lattice, Cambridge University Press, 1997.
[3] George F. Sterman, Paul Stoler, Annu. Rev. Nucl. Part. Sci. 47 (1997) 193.
[4] A.H. Mueller, Nucl. Phys. A 654 (1999) 37C.
[5] S.R. Beane, W. Detmold, K. Orginos, M.J. Savage, Prog. Part. Nucl. Phys. 66 (2011) 1.
[6] I.C. Cloët, C.D. Roberts, Prog. Part. Nucl. Phys. 77 (2014) 1.
[7] S.J. Brodsky, H.-C. Pauli, S.S. Pinsky, Phys. Rep. 301 (1998) 299.
[8] J.P. Vary, Nucl. Phys. Proc. Suppl. 251–252 (2014) 155.
[9] D. Chakrabarti, X. Zhao, H. Honkanen, R. Manohar, P. Maris, J.P. Vary, Phys. Rev. D 89 (2014) 116004.
[10] P. Wiecki, Y. Li, X. Zhao, P. Maris, J.P. Vary, Phys. Rev. D 91 (2015) 105009.
[11] P. Wiecki, Y. Li, X. Zhao, P. Maris, J.P. Vary, Few-Body Syst. 56 (2015) 489.
[12] Y. Li, V.A. Karmanov, P. Maris, J.P. Vary, Few-Body Syst. 56 (2015) 495.
[13] Y. Li, P. Maris, X. Zhao, J.P. Vary, Phys. Lett. B 758 (2016) 118.
[14] L. Adhikari, Y. Li, X. Zhao, P. Maris, J.P. Vary, A.A. El-Hady, Phys. Rev. C 93 (2016) 055202.
[15] W. Broniowski, S. Prelovsek, L. Santelj, E. Ruiz Arriola, Phys. Lett. B 686 (2010) 313.
[16] A.E. Dorokhov, W. Broniowski, E. Ruiz Arriola, Phys. Rev. D 84 (2011) 074015.
[17] F. Gross, Phys. Rev. 186 (1969) 1448.
[18] E.P. Biernat, F. Gross, T. Peña, A. Stadler, Phys. Rev. D 89 (2014) 016005.
[19] E.P. Biernat, F. Gross, T. Peña, A. Stadler, Few-Body Syst. 55 (2014) 705.
[20] M.T. Peña, S. Leitão, E.P. Biernat, A. Stadler, J.E. Ribeiro, F. Gross, Few-Body Syst. 57 (2016) 467.
[21] E.P. Biernat, F. Gross, T. Peña, A. Stadler, Phys. Rev. D 89 (2014) 016006.
[22] E.P. Biernat, F. Gross, M.T. Peña, A. Stadler, Phys. Rev. D 92 (2015) 076011.
[23] H.-M. Choi, C.-R. Ji, Z. Li, H.-Y. Ryu, Phys. Rev. C 92 (2015) 055203.
[24] S. Noguera, S. Scopetta, J. High Energy Phys. 11 (2015) 102.
[25] M.V. Terentév, Sov. J. Nucl. Phys. 24 (1976) 106;
L.A. Kondratyuk, M.V. Terentév, Sov. J. Nucl. Phys. 31 (1980) 561.
[26] T. Frederico, G.A. Miller, Phys. Rev. D 45 (1992) 4207;
Phys. Rev. D 50 (1994) 210.
[27] J.P.B.C. de Melo, T. Frederico, Phys. Rev. C 55 (1997) 2043.
[28] B.L.G. Bakker, H.-M. Choi, C.-R. Ji, Phys. Rev. D 65 (2002) 116001.
[29] C.S. Mello, A.N. da Silva, J.P.B.C. de Melo, T. Frederico, Few-Body Syst. 56 (2015) 509.
[30] J.P.B.C. de Melo, H.W.L. Naus, T. Frederico, Phys. Rev. C 59 (1999) 2278.
[31] J.P.B.C. de Melo, T. Frederico, E. Pace, G. Salmé, Nucl. Phys. A 707 (2002) 399; Braz. J. Phys. 33 (2003) 301.
[32] E.O. da Silva, J.P.B.C. de Melo, B. El-Bennich, V.S. Filho, Phys. Rev. C 86 (2012) 038202.
[33] G.H.S. Yabusaki, I. Ahmed, M. Ali Paracha, J.P.B.C. de Melo, B. El-Bennich, Phys. Rev. D 92 (2015) 034017.
[34] B.L.G. Bakker, H.-M. Choi, C.-R. Ji, Phys. Rev. D 67 (2003) 113007.
[35] T. Frederico, E. Pace, B. Pasquini, G. Salmè, Phys. Rev. D 80 (2009) 054021.
[36] C. Fanelli, E. Pace, G. Romanelli, G. Salmè, M. Salmistraro, Eur. Phys. J. C 76 (2016) 253.
[37] M.B. Parappilly, P.O. Bowman, U.M. Heller, D.B. Leinweber, A.G. Williams, J.B. Zhang, Phys. Rev. D 73 (2006) 054504.
[38] L. Chang, I.C. Cloët, J.J. Cobos-Martinez, C.D. Roberts, S.M. Schmidt, P.C. Tandy, Phys. Rev. Lett. 110 (2013) 132001.
[39] I.C. Cloët, L. Chang, C.D. Roberts, S.M. Schmidt, P.C. Tandy, Phys. Rev. Lett. 111 (2013) 092001.
[40] L. Chang, I.C. Cloët, C.D. Roberts, S.M. Schmidt, P.C. Tandy, Phys. Rev. Lett. 111 (2013) 141802.
[41] C. Itzykson, J.-B. Zuber, Quantum Field Theory, McGraw-Hill, 1980.
[42] N. Nakanishi, Graph Theory and Feynman Integrals, Gordon and Breach, New York, 1971.
[43] D. Dudal, O. Oliveira, P.J. Silva, Phys. Rev. D 89 (2014) 014010.
[44] S. Strauss, C.S. Fischer, C. Kellermann, Phys. Rev. Lett. 109 (2012) 252001.
[45] J. Carbonell, V.A. Karmanov, Eur. Phys. J. A 27 (2006) 1.
[46] T. Frederico, G. Salmè, M. Viviani, Phys. Rev. D 89 (2014) 016010.
[47] J. Carbonell, V.A. Karmanov, Eur. Phys. J. A 46 (2010) 387.
[48] T. Frederico, G. Salmè, M. Viviani, Phys. Rev. D 85 (2012) 036009.
[49] T. Frederico, G. Salmè, M. Viviani, Eur. Phys. J. C 75 (2015) 398.
[50] C. Gutierrez, V. Gigante, T. Frederico, G. Salmè, M. Viviani, L. Tomio, Phys. Lett. B 759 (2016) 131.
[51] E. Rojas, J.P.B.C. de Melo, B. El-Bennich, O. Oliveira, T. Frederico, J. High Energy Phys. 1310 (2013) 193.
[52] D. Dudal, M.S. Guimarães, L.F. Palhares, S.P. Sorella, Ann. Phys. 365 (2016) 155.
[53] C.S. Fischer, R. Alkofer, Phys. Rev. D 67 (2003) 094020.
[54] R. Alkofer, W. Detmold, C.S. Fischer, P. Maris, Phys. Rev. D 70 (2004) 014014.
[55] J. Greensite, Lect. Notes Phys. 821 (2011) 1.
[56] J.P.B.C. de Melo, T. Frederico, E. Pace, G. Salmè, Phys. Lett. B 581 (2004) 75.
[57] J.P.B.C. de Melo, T. Frederico, E. Pace, G. Salmè, Phys. Rev. D 73 (2006) 074013.
[58] C. Lorcé, B. Pasquini, P. Schweitzer, Eur. Phys. J. C 76 (2016) 415.
[59] H. Pagels, S. Stokar, Phys. Rev. D 20 (1979) 2947.
[60] J.M. Cornwall, Phys. Rev. D 22 (1980) 1452.
[61] H. Pagels, S. Stokar, Phys. Rev. D 22 (1980) 2876.
[62] J.M. Cornwall, Phys. Rev. D 26 (1982) 1453.
[63] J.C. Ward, Phys. Rev. 78 (1950) 182.
[64] Y. Takahashi, Nuovo Cimento 6 (1957) 371.
[65] M.E. Peskin, D.V. Schroeder, An Introduction to Quantum Field Theory, Addison–Wesley, Reading, USA, 1995, p. 842.
[66] H.-M. Choi, C.-R. Ji, Phys. Rev. D 91 (2015) 014018.
[67] K.A. Olive, et al., Particle Data Group, Chin. Phys. C 38 (2014) 090001, and 2015 update.
[68] R. Tarrach, Z. Phys. C 2 (1979) 221.
[69] S.B. Gerasimov, Sov. J. Nucl. Phys. 29 (1979) 259;
S.B. Gerasimov, Sov. J. Nucl. Phys. 32 (1980) 156 (Erratum).
[70] S.R. Amendolia, et al., Phys. Lett. B 146 (1984) 116.
[71] R. Baldini, E. Pasqualucci, S. Dubnicka, P. Gauzzi, S. Pacetti, Y. Srivastava, Nucl. Phys. A 666 (2000) 38.
[72] J. Volmer, et al., Phys. Rev. Lett. 86 (2001) 1713.
[73] T. Horn, et al., Phys. Rev. Lett. 97 (2006) 192001.
[74] V. Tadevosyan, et al., Phys. Rev. C 75 (2007) 055205.
[75] G.M. Huber, et al., Phys. Rev. C 78 (2008) 045203.
[76] T. Frederico, G. Salmè, Few-Body Syst. 49 (2011) 163.